Supplementary Information

High Faraday efficiency of Cu_1Co_1-BCN based on Dodecahydro-*Closo*-Dodecaborate Hybrid for electrocatalytic reduction of nitrate to ammonia

Jiajia Wang[#a,b], Zhengyu Fan[#b], Haixu Zhao[b], Xun Liu[b], Mai Zheng[b], Long Zhang[a,*], Yingtang Zhou[c,*], Lijie Sun[d], Jinghuan Liu[d,e], Haibo Zhang[b,*]

[a] *School of Optoelectronic Materials and Technology, Jianghan University, Wuhan, 430056, China.*

[b] *College of Chemistry and Molecular Sciences; Engineering Research Center of Organosilicon Compounds & Materials, Ministry of Education, Wuhan University, Wuhan, 430072, China.*

[c] *National Engineering Research Center for Marine Aquaculture, Marine Science and Technology College Zhejiang Ocean University, Zhoushan, 316004, China*

[d] *Shijiazhuang Siyao Co., Ltd, Shijiazhaung, 050000, China*

[e] *College of Pharmacy, Hebei Medical University, Shijiazhaung, 050000, China*

E-mail addresses: lzh131@jhun.edu.cn (L. Zhang), zhouyingtang@zjou.edu.cn(Y.Zhou）,

haibozhang1980@gmail.com (H.B Zhang)

Jiajia Wang and zhengyu Fan contributed equally to this work.

Contents

Texts

Text S1. Chemical and materials

Text S2. Material characterization methods

Text S3. Product detection method

Text S4. DFT calculations

Figures

Fig. S1. (a)The SEM images of Cu-BCN and (b) Cu_1Co_1-BCN.

Fig. S2. (a) The Cu 2p spectrum of Cu-BCN and (b) Cu_1Co_1-BCN, XPS spectrum and (c) Auger spectrum of Cu in Cu_1Co_1-BCN.

Fig. S3. The LSV curve when the electrolyte with NO_3^- and without NO3-, where (a) Cu-BCN, Cu_2Co_1-BCN, Cu_1Co_1-BCN and Cu_1Co_2-BCN as working electrode.

Fig. S4. Current-time curve under different applied potentials (Cu-BCN as working electrode).

Fig. S5. The standard curve of (a) NH_4^+, (b) NO_2^- and (c) NO_3^-.

Fig. S6. (a) The Faraday efficiency and the rate of ammonia production, (b) ratio of Faraday efficiency of Cu-BCN, the Faraday efficiency and the rate of NO_2^- production (c) Cu-BCN, (d) Cu_1Co_1-BCN.

Fig. S7. Ammonia yield with and without nitrate at -0.5 V vs. RHE when Cu_1Co_1-BCN as catalyst.

Text S1. Chemical and materials

All reagents were used without any further purification. All the chemicals were of analytical grade and were used as received without further purification. The reagents were purchased from Aladdin Chemical Reagent Co., Ltd. Nafion 117 proton exchange membrane was purchased from Shanghai Hesen Electric Co., Ltd. Hydrophilic carbon paper (CP) was purchased from Shanghai Hesen Electric Co., Ltd.

Text S2. Material characterization methods

The morphology of the synthesized Cu_xCo_y-BCN was examined with scanning electron microscopy (SEM, HITACHI SU8010, Japan). The elemental mapping, HRTEM images were explored by a JEM-2100F electron microscope (JEOL, Japan HITACHI). The chemical functional groups were investigated by Fourier transformed infrared spectroscopy (FTIR, Nicolet6700, Thermo Scientific, USA). X-ray diffraction (XRD) patterns were recorded with Cu Kα radiation (Empyrean, PANalytical B. V.). X-Ray photoelectron spectra (XPS) were collected by a Thermo ESCALAB 250xi X-ray photoelectron spectrometer with Al Kα X-ray (1486.6 eV) as the excitation source.

Text S3. Product detection method

3.1 The detection of NH_4^+-N yields:

Detection of NH_4^+-N was performed using indophenol blue colorimetry: six standard solution gradients of 0.1 μg/mL, 0.4 μg/mL, 0.8 μg/mL, 1.6 μg/mL, 2.5 μg/mL, 4 μg/mL of NH_4Cl in 0.1 M KOH solution were prepared. Adding 0.2 mL of 1 wt% sodium nitroprusside solution, 2 mL of 1 M NaOH solution (containing 5 wt% salicylic acid and 5 wt% sodium citrate), and 1 mL of 0.05 M NaClO solution (to be used as needed) to 2 mL gradient standard solutions. After standing for 2 h, the absorbance at 657 nm was recorded on the ultraviolet spectrophotometer, and the standard curve line was drawn according to the correlation between the absorbance of the ultraviolet spectrophotometer and the concentration of NH_4^+-N solution.

3.2 The detection of NO_2^--N yields:

Detection of NO_2^--N by colorimetric method. 0.1 g of N-(1-naphthyl)-ethylenediamine hydrochloride, 1.0 g of sulfonamide and 2.94 mL of phosphoric acid were dissolved in 50 mL of deionized water to form Griess color developer. Six standard solutions were prepared in 0.1 M KOH solution at 0.4 μg/mL, 0.8 μg/mL, 1 μg/mL, 1.6 μg/mL, 3.2 μg/mL, 6.4 μg/mL and 6.4 μg/mL of

$NaNO_2$ solution. 1 mL of gradients of standard solutions was added to 2 mL of water with 1 mL of Griess colorant. After standing for 10 minutes for color development, the absorbance value at 540 nm was recorded on the UV-visible spectrophotometer, and the standard curve was drawn according to the relationship between absorbance and NO_2^--N solution concentration.

3.3 The detection of NO_3^--N yields:

Detection of NO_3^--N by colorimetric method. Six standard solutions (0.5 μg/mL, 1 μg/mL, 1.5 μg/mL, 2 μg/mL, 2.5 μg/mL, and 3 μg/mL) were prepared in 0.1 M KOH solution. The 2 mL standard solution, 1 mL 1 M HCl solution and 0.1 mL 0.8 wt% sulfamic acid solution were mixed. After standing for 30 minutes, the absorbance value at 208 nm was recorded on the UV-visible spectrophotometer, and the standard curve was drawn according to the relationship between the concentration gradient and absorbance.

Text S4. DFT calculations

All of the spin-polarized DFT calculations were performed with the projector augmented plane-wave method based on MeadA platform, as implemented in the Vienna ab initio simulation package. The generalized gradient approximation proposed by Perdew-Burke-Ernzerhof is selected for the exchange-correlation potential. The Cu-BCN and Cu_1Co_1-BCN crystal structure has been modeled using a single periodic slab with a (2 x 2) and (2 x 1) super cell. The Cu (111) facet and Co (101) facet were investigated which was dominant facet according to the HTEM patterns, respectively. The suitable vacuum layers were set to 15 Å, in order to avoid the interaction between periodic structures. The cut-off energy for plane wave is set to 500 eV. The energy criterion is set to 10^{-5} eV in iterative solution of the Kohn-Sham equation. The Brillouin zone integration is performed using a 1 × 2 × 2 k-mesh. The slab contains four layers with two layers are fixed. All the structures are relaxed until the residual forces on the atoms have declined to less than 0.05 eV/Å.

The free energy of adsorbed and non-adsorbed substances is calculated as below：

$$\Delta G_{ads} = \Delta E + \Delta E_{ZPE} - T\Delta S \quad (1)$$

where ΔEads, ΔEZPE, T, and ΔS, represent adsorption energy, zero-point energy, temperature, and entropy change, respectively. In order to describe charged NO_3^- (as a reference), a neutral HNO_3 gas was selected as a substitute for NO_3^- and the energy of NO_3^- was obtained in the thermodynamic cycle to avoid the difficulty of periodic DFT calculations for charged systems.

The free energy of the intermediate H* state (ΔGH*) is considered to be a key indicator of the

HER activity of the electrocatalyst. According to Eq.1,

$$\Delta S = SH^* - 1/2S(H_2) \approx -1/2S(H_2) \quad (2)$$

where $S_{(H2)}$ is the entropy of $H_2(g)$ under standard conditions. Thus, ΔE can be calculated as follows:

$$\Delta E_{H^*} = E_{(sub+H^*)} - E_{(sub)} - 1/2E_{(H2)} \quad (3)$$

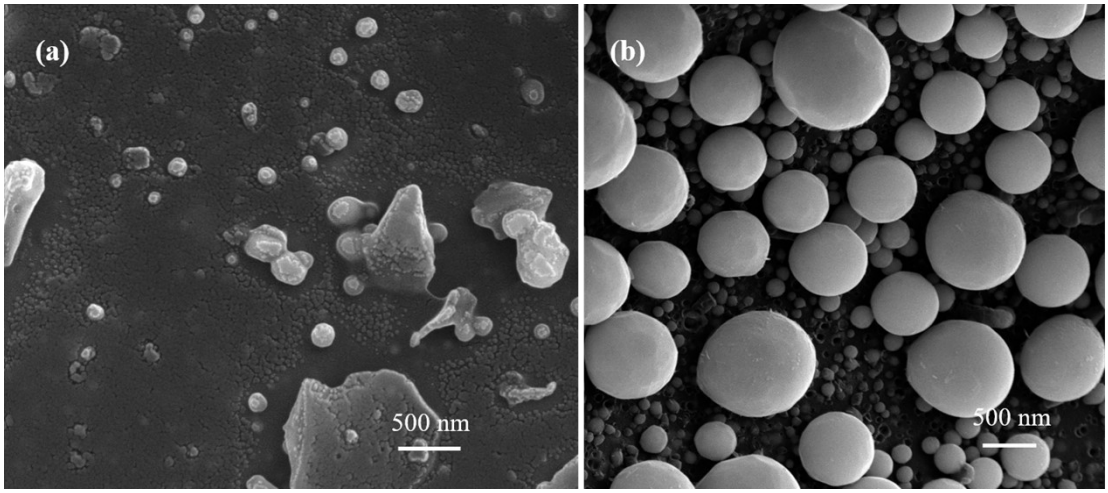

Fig. S1. (a)The SEM images of Cu-BCN and (b) Cu_1Co_1-BCN.

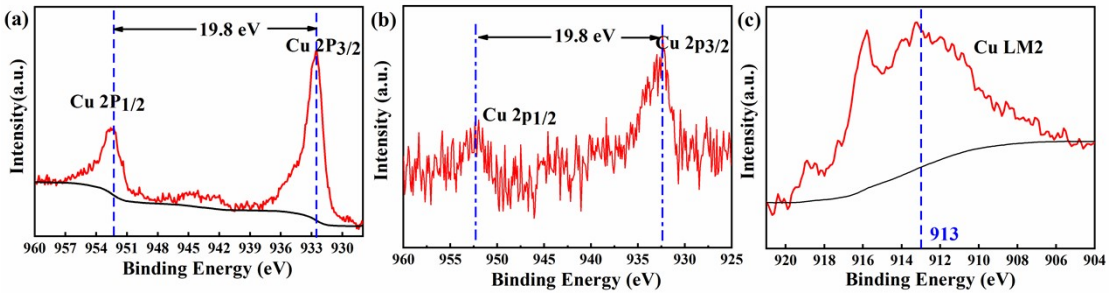

Fig. S2. (a) The Cu 2p spectrum of Cu-BCN and (b) Cu_1Co_1-BCN, XPS spectrum and (c) Auger spectrum of Cu in Cu_1Co_1-BCN.

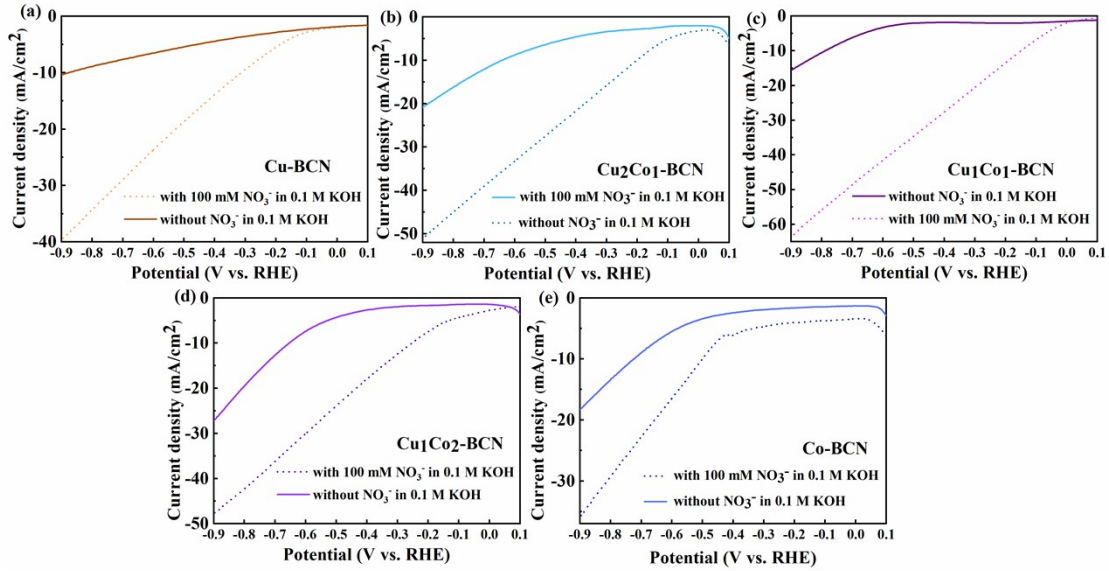

Fig. S3. The LSV curve when the electrolyte with NO_3^- and without NO_3^-, where (a) Cu-BCN, (b) Cu_2Co_1-BCN, (c) Cu_1Co_1-BCN, (d) Cu_1Co_2-BCN and (e) Co-BCN as working electrode.

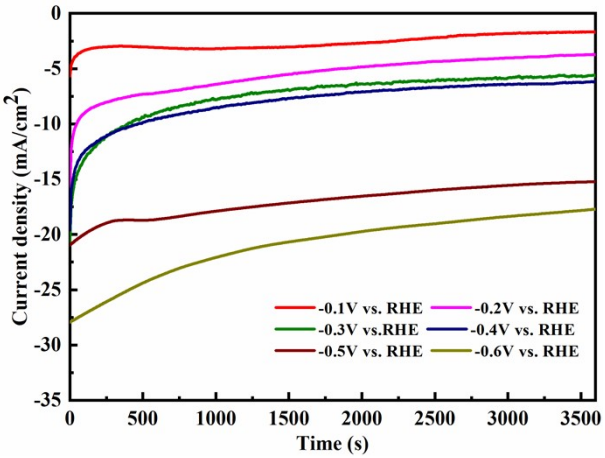

Fig. S4. Current-time curve under different applied potentials (Cu-BCN as working electrode).

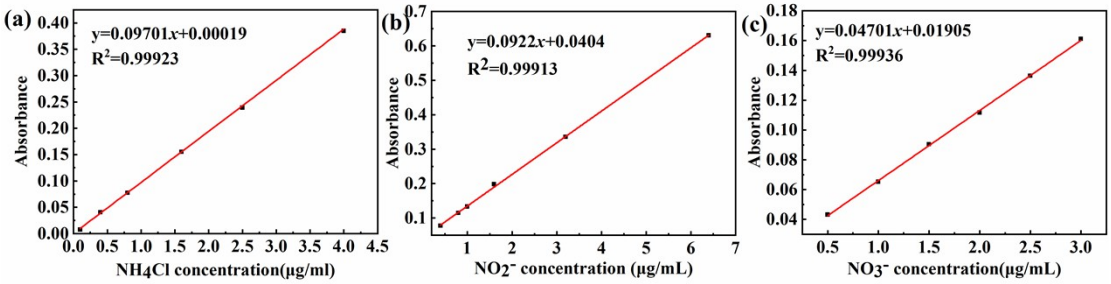

Fig. S5. The standard curve of (a) NH_4^+, (b) NO_2^- and (c) NO_3^-.

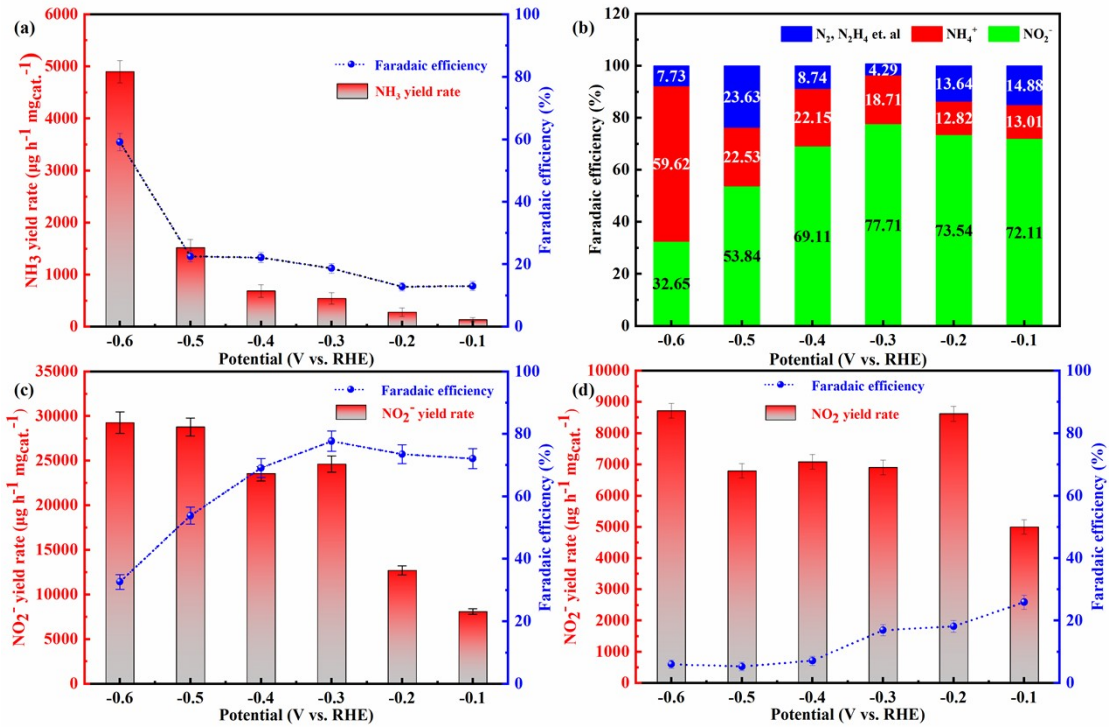

Fig. S6. (a) The Faraday efficiency and the rate of ammonia production, (b) ratio of Faraday efficiency of Cu-BCN, the Faraday efficiency and the rate of NO_2^- production (c) Cu-BCN, (d) Cu_1Co_1-BCN.

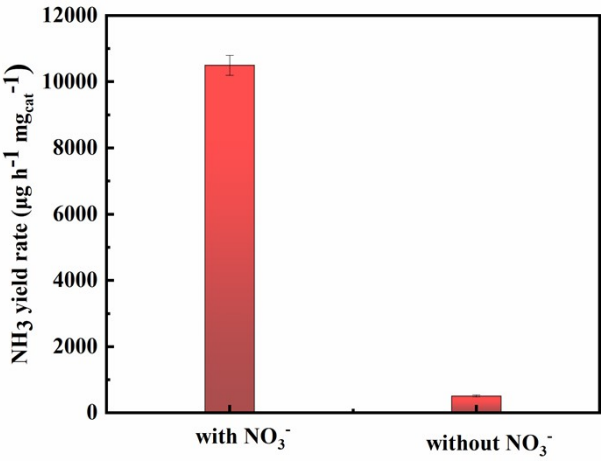

Fig. S7. Ammonia yield with and without nitrate at -0.5 V vs. RHE when Cu_1Co_1-BCN as catalyst.